

See discussions, stats, and author profiles for this publication at: <https://www.researchgate.net/publication/245211180>

UV-induced unimolecular photochemistry of 2(5 H)-furanone and 2(5 H)-thiophenone isolated in low temperature inert matrices

ARTICLE *in* VIBRATIONAL SPECTROSCOPY · MAY 2009

Impact Factor: 2 · DOI: 10.1016/j.vibspec.2008.07.015

CITATIONS

7

READS

26

3 AUTHORS:



S. Breda

University of Coimbra

17 PUBLICATIONS 258 CITATIONS

SEE PROFILE



Igor D. Reva

University of Coimbra

126 PUBLICATIONS 2,549 CITATIONS

SEE PROFILE

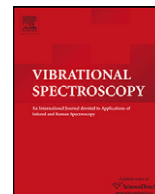


Rui Fausto

University of Coimbra

330 PUBLICATIONS 4,517 CITATIONS

SEE PROFILE



UV-induced unimolecular photochemistry of 2(5H)-furanone and 2(5H)-thiophenone isolated in low temperature inert matrices

S. Breda^{*}, I. Reva, R. Fausto

Department of Chemistry, University of Coimbra, 3004-535 Coimbra, Portugal

ARTICLE INFO

Article history:

Received 1 February 2008

Received in revised form 23 July 2008

Accepted 28 July 2008

Available online 19 August 2008

Keywords:

Matrix-isolation

Infrared spectroscopy

Photochemistry

2(5H)-furanone

2(5H)-thiophenone

Aldehyde-ketene

Thioaldehyde-ketene

Dewar isomer

ABSTRACT

Monomers of two simplest five-membered heterocyclic α -carbonyl compounds, 2(5H)-furanone and 2(5H)-thiophenone were isolated in low temperature inert argon matrices and their UV-induced photochemistry was studied. The reaction photoproducts were identified by FTIR spectroscopy and interpretation of the experimental results was assisted by theoretical calculations of the infrared spectra at the DFT(B3LYP)/6-311++G(*d,p*) level. Both compounds were found to undergo UV-induced α -cleavage photoreaction, however at different excitation wavelengths. The open ring aldehyde-ketene was generated from 2(5H)-furanone upon UV irradiation with $\lambda > 235$ nm light, while 2(5H)-thiophenone reacted at lower excitation energies ($\lambda > 285$ nm) with formation of thioaldehyde-ketene. At higher excitation energies ($\lambda > 235$ nm), thioaldehyde-ketene was transformed into the Dewar isomer and subsequently decomposed with formation of carbonyl sulphide, while aldehyde-ketene did not react any further. The different photochemical reactivity experimentally observed for the two families of compounds was explained on the basis of the natural bond orbital analysis carried out at the MP2/6-311++G(*d,p*) level of theory.

© 2008 Elsevier B.V. All rights reserved.

1. Introduction

Recently, the structure and vibrational spectra of two five-membered heterocyclic α -carbonyl compounds, 2(5H)-thiophenone and 2(5H)-furanone (Scheme 1), have been studied in our laboratory [1]. The experimental FTIR spectra of the monomers of these compounds isolated in inert argon matrices at 10 K were investigated, the interpretation of the experimental data being supported by vibrational calculations at the MP2 and DFT(B3LYP)/6-311++G(*d,p*) levels of theory. Spectra/structure correlations were obtained for both compounds and for their six-membered ring analogues, thiapyran-2-one and α -pyrone. Natural bond orbital (NBO) analysis was also undertaken on the two studied compounds, revealing important details of their electronic structure and dominant intramolecular interactions, and providing an additional way of interpreting some of the most significant features of their vibrational spectra.

The objective of the present work is the characterization of the photochemistry of these two molecules isolated in low temperature rare gas matrices.

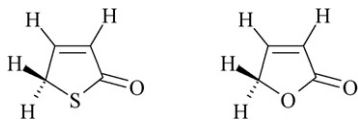
The photochemistry of five-membered heterocyclic α -carbonyl compounds in different solutions was studied by several authors

for a long time [2–5]. Margaretha and co-workers [6–17] reported that upon irradiation 2(5H)-thiophenones behave quite differently from the corresponding oxygen-based heterocycles. While 2(5H)-furanones exhibit a typical enone-like behaviour, giving rise to cyclic dimers, [2 + 2] cycloadducts with alkenes or photoreduced products (e.g., saturated lactones) in alcoholic solutions via triplet state [16,18], the unsaturated thiolactones undergo ring opening to α,β -unsaturated mercapto esters via singlet state. On the other hand, it has also been shown that, like furanones, thiophenones can also undergo [2 + 2] photocycloadditions with alkenes in cyclohexane solution [11]. Interestingly, in all above mentioned studies, furanones and thiophenones were involved in cross-reactions with the solvent, whereas the photochemical behaviour of the isolated compounds (either in gaseous phase or in inert matrices), as far as we know, was not reported hitherto.

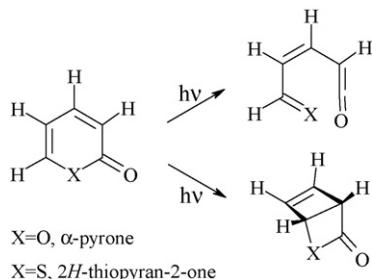
Recently, we have studied the photochemistry of matrix-isolated analogues of 2(5H)-thiophenone and 2(5H)-furanone, six-membered heterocyclic α -carbonyl compounds 2H-thiopyran-2-one [19], α -pyrone [20] and some of their derivatives [21,22]. In these studies we showed that monomers of these compounds exhibit various reaction photochannels, whose relative yield can be modulated by changing the irradiation wavelength or substituents present in the ring. Such investigations allowed the successful identification of a number of reaction intermediates and final products. In these molecules, two main competitive photochemical reaction pathways were identified: ring-opening, leading

^{*} Corresponding author.

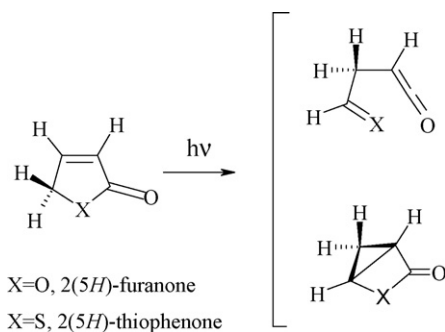
E-mail address: sbreda@qui.uc.pt (S. Breda).



Scheme 1. Schematic representation of 2(5H)-thiophenone (left) and 2(5H)-furanone (right).



Scheme 2. Two main photochemical reaction pathways observed for six-membered heterocyclic α -carbonyl compounds (α -pyrone and 2H-thiopyran-2-one): ring-opening, leading to formation of the isomeric aldehyde-ketene or thioaldehyde-ketene, and ring-contraction leading to the corresponding Dewar isomers [19,20].



Scheme 3. Ring-opening and ring-contraction reactions in furanone and thiophenone. Note the necessary occurrence of a [1,2]-hydrogen atom migration during these reactions.

to formation of the isomeric aldehyde-ketenes, and ring-contraction resulting in the Dewar isomers (Scheme 2).

For five-membered compounds, by analogy with the six-membered heterocycles, both the ring-opening and the ring-contraction reactions can also be conceived. However they would require the simultaneous occurrence of an intramolecular [1,2]-hydrogen shift (Scheme 3). This requirement could be expected to introduce important differences in the reactivity of the two types of compounds.

In the present work the photochemical study of 2(5H)-thiophenone and 2(5H)-furanone isolated in an Ar matrix is reported. The characterization of the photoproducts of unimolecular reactions has been carried out experimentally, using the low temperature matrix-isolation technique combined with FTIR spectroscopy, as well as theoretically, applying high-level quantum chemistry calculations.

2. Experimental

Commercial samples of 2(5H)-thiophenone (Aldrich, 98%) and 2(5H)-furanone (Aldrich, 98%) were used in this investigation. The experimental apparatus and procedures are described elsewhere [1]. The chosen compound was placed in a glass ampoule protected against light and connected to the sample chamber of an APD Cryogenics DE-202A closed-cycle helium cryostat through a NUPRO SS-4BMRG needle valve with shut-off possibility. Prior

to the experiment, the compound was purified from dissolved gases by the multiple freeze–pump–thaw procedure, using the vacuum system of the cryostat. Two parts of the effusive cell, the valve nozzle and the sample compartment, were thermostatted separately. During deposition, the valve nozzle was kept at room temperature, while the sample compartment was cooled to -50°C , by immersing the ampoule with the compound in a bath with melting *sec*-amyl alcohol. This allowed the saturated vapour pressure over the compound to be reduced and the metering function of the valve to be improved. The vapour of furanone (or thiophenone) was introduced into the cryostat chamber together with large excess of the host matrix gas (argon N60, Air Liquide) coming from a separate line. The argon flux was controlled using the standard manometric procedure.

A cold CsI window mounted on the tip of the cryostat was used as the optical substrate. The sample compartment of the spectrometer was modified in order to couple it with the cryostat head and allow purging of the instrument by a stream of dry nitrogen to remove water vapour and CO_2 .

The matrices were irradiated through the outer KBr window of the cryostat, with filtered or unfiltered light from a 500 W Hg(Xe) lamp (Spectra-Physics, model no. 66142) adjusted to provide 200 W output power. In the course of experiment, temperature of the samples was measured directly at the sample holder by a silicon diode sensor connected to a digital controller (Scientific Instruments, Model 9650-1) and did not exceed 12 K.

The infrared spectra were recorded in the $4000\text{--}400\text{ cm}^{-1}$ spectral region, with 0.5 cm^{-1} resolution, using a Mattson (60AR) Infinity Series FTIR spectrometer equipped with a KBr beamsplitter and a DTGS detector. The experimental spectra were averaged after 256 scans.

3. Computational

The equilibrium geometries for all studied species were fully optimized at the DFT and MP2 levels of theory with the standard 6-311++G(d,p) basis set. The DFT calculations were carried out with the B3LYP density functional, which includes Becke's [23] gradient exchange correction, and the Lee et al. [24] and the Vosko et al. [25] correlation functionals. No restriction of symmetry was imposed on the initial structures.

The nature of the obtained stationary points on the potential energy surfaces of the studied systems was checked through the analysis of the corresponding Hessian matrix. A set of internal coordinates was defined and the Cartesian force constants were transformed to the internal coordinates space, allowing ordinary normal-coordinate analysis to be performed as described by Schahtschneider and Mortimer [26]. The calculated harmonic frequencies were also used to assist the analysis of the experimental spectra (scaled with a factor of 0.978) and to account for the zero-point vibrational energy (ZPVE) corrections (non-scaled).

All calculations in this work were done using the Gaussian 03 program [27].

The specific nature of the electronic structures in the studied compounds was characterized by natural bond orbital (NBO) analysis [28,29], using NBO version 3, as implemented in Gaussian 03.

4. Results and discussion

4.1. Effect of UV irradiation on matrix-isolated 2(5H)-thiophenone

The infrared spectrum of 2(5H)-thiophenone (or, for brevity, thiophenone) monomers isolated in argon matrix was reported in our previous study [1]. The experimental data were compared with

results of theoretical simulations carried out at the DFT(B3LYP) and MP2/6-311++G(d,p) levels of approximation. A very good agreement between the experimental and theoretical spectra allowed for the full assignment of the observed bands.

After isolation of thiophenone monomers in an argon matrix, the sample was subjected to a series of UV-irradiations with different longpass filters, gradually decreasing cut-off wavelength, and thus increasing the transmitted UV-energy. As for the previously studied six-membered heterocyclic α -carbonyl compounds [19–22,30], a dependence on the irradiation wavelength was found. The absorptions due to thiophenone started to decrease and new absorptions appeared in the spectrum of the irradiated sample when the cutoff wavelength was decreased to 285 nm. At this wavelength, a series of irradiations was carried out, with different expositions, starting from 5 min and up to 60 min (total) of irradiation. At different periods of such irradiation, all the photoproduct bands showed the same relative kinetics. Upon 60 min of irradiation, the total of ca. 85% of the reagent was consumed (see Fig. 1).

After 60 min of UV ($\lambda > 285$ nm) irradiation, the characteristic intense, structured band due to the antisymmetric stretching vibration (ca. 2140–2125 cm^{-1} [19–22,31,32]) of ketene group ($\text{C}=\text{C}=\text{O}$) appears in the spectrum of the irradiated sample, thus providing evidence for the generation of the thioaldehyde-ketene (T) resulting from the ring-opening photoreaction.

The T species has two intramolecular rotational degrees of freedom (see Scheme 3), which correspond to rotations of

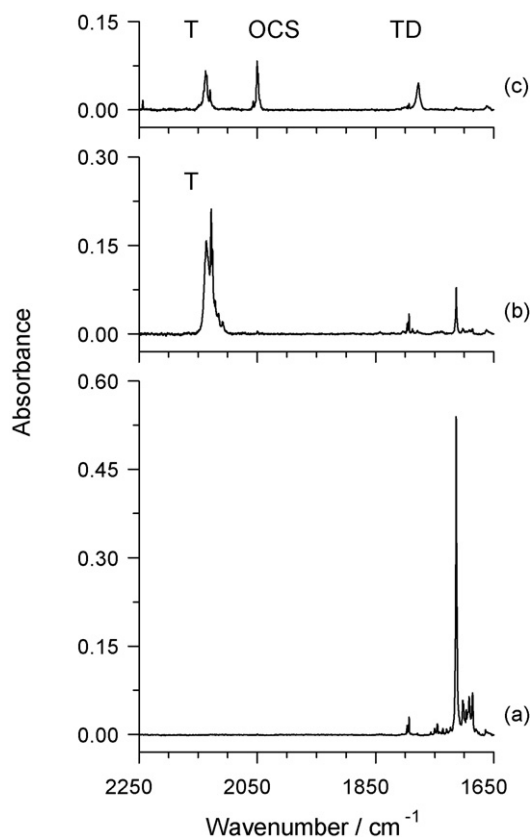


Fig. 1. Region 2200–1650 cm^{-1} of the observed infrared spectrum of 2(5H)-thiophenone isolated in argon matrix (10 K): (a) as-deposited matrix; (b) after 60 min of UV ($\lambda > 285$ nm) irradiation and, (c) after subsequent 30 min UV ($\lambda > 235$ nm) irradiation. Features due to the products of reaction marked with “T”, “OCS” and “TD” correspond to open-ring thioaldehyde-ketene, carbonyl sulphide ($\text{O}=\text{C}=\text{S}$) and Dewar isomer of thiophenone (see text). The small band just below 1800 cm^{-1} in spectra (a) and (b) is due to absorption of 2(5H)-furanone monomers present in the sample as a vestigial impurity.

the $\text{C}=\text{C}=\text{O}$ and $\text{CH}=\text{S}$ groups with respect to each other, and can then exist in different conformations. In order to obtain the structures of these forms, the two conformationally relevant dihedral angles ($\text{C}=\text{C}-\text{C}-\text{C}$ and $\text{C}-\text{C}-\text{C}=\text{S}$) were incrementally changed in steps of 5° and all remaining coordinates were optimized. The obtained potential energy surface (PES) is depicted in Fig. S2 (supplementary material). Seven minima were found on the PES of the compound, corresponding to four different conformers (T1, T2, T3 and T4), with all but T3 being doubly degenerated by symmetry. The optimized structures for the four different conformers, their symmetry, dipole moment and relative energies are given in Table 1.

In the most stable conformer (T1), the thioaldehyde and ketene groups adopt an approximately anti-parallel configuration, with the $\text{C}=\text{C}-\text{C}-\text{C}$ and $\text{C}-\text{C}-\text{C}=\text{S}$ dihedral angles equal to 112.4° and 119.1° . This geometric arrangement provides the maximal distance between the fractionally charged groups, with the positively charged hydrogen atoms linked to the thioaldehyde and ketene groups (as well as the negatively charged thioaldehyde and ketene heteroatoms) pointing in opposite directions. Accordingly, this structure has the smallest dipole moment among all the open-ring conformers (see Table 1). The second most stable form (T2) is predicted to be 2.3 kJ mol^{-1} higher in energy than T1. In T2, the ketene and thioaldehyde groups are nearly perpendicular to each other, the $\text{C}=\text{C}-\text{C}-\text{C}$ and $\text{C}-\text{C}-\text{C}=\text{S}$ angles being 141.4° and 3.6° , respectively. The third conformer in order of increasing energies (T3) has C_s symmetry and both conformationally relevant dihedral angles equal to 0° , being the sole form which does not have a symmetry equivalent structure. This is the conformer which has the largest dipole moment and has an energy 3.0 kJ mol^{-1} higher than that of T1. Finally, in the fourth conformer (T4) the thioaldehyde and ketene groups adopt a configuration approximately parallel, with $\text{C}=\text{C}-\text{C}-\text{C}$ and $\text{C}-\text{C}-\text{C}=\text{S}$ dihedral angles of 99.6° and -126.0° , corresponding to the highest energy conformer of the molecule, with a relative energy of 3.1 kJ mol^{-1} . When the zero-point energy corrections are taken into account, the relative energies of T2, T3 and T4 amount to 1.0, 1.5 and 2.8 kJ mol^{-1} (see Table 1), respectively.

The potential energy profiles for interconversion between the conformers are presented in Fig. 2. As stressed in this figure,

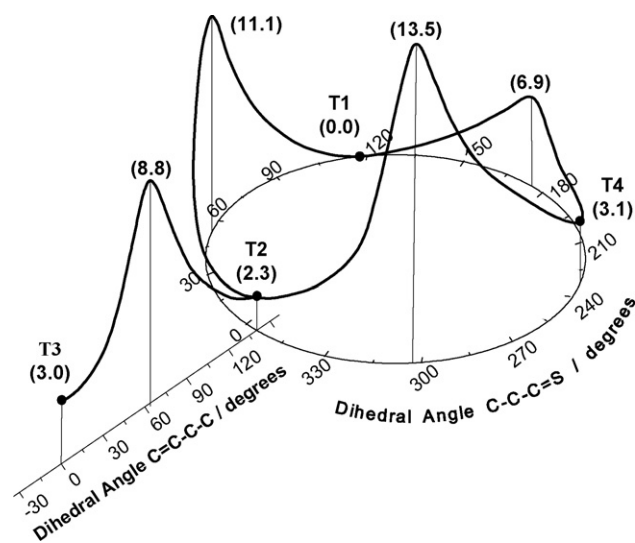


Fig. 2. Calculated potential energy profiles [DFT(B3LYP)/6-311++G(d,p)] for interconversion between the different conformers of thioaldehyde-ketene opening isomer of thiophenone. Relative energies (kJ mol^{-1} , with respect to form T1) for the stationary points (minima and saddle points on the PES) are given in parentheses.

Table 1
DFT(B3LYP)/6-311++G(d,p) calculated relative energies (ΔE° , kJ mol⁻¹), zero-point vibrational energy corrected relative energies ($\Delta E^\circ_{\text{ZPVE}}$, kJ mol⁻¹), dipole moments ($|\mu|$, debye), conformer defining dihedral angles (degrees) and symmetry point group of the thioaldehyde-ketene (T) conformers^a

Conformer	Dihedral angle	Symmetry	ΔE°	$\Delta E^\circ_{\text{ZPVE}}$	$ \mu $
T1	C=C–C–C: 112.4	C ₁	0.0	0.0	0.95
T2	C–C–C=S: 119.1 C=C–C–C: 141.4	C ₁	2.3	1.0	2.24
T3	C–C–C=S: 3.6 C=C–C–C: 0.0	C _s	3.0	1.5	3.85
T4	C–C–C=S: 0.0 C=C–C–C: 99.6	C ₁	3.1	2.8	2.85
	C–C–C=S: –126.0				

^a The calculated values of E° and E°_{ZPVE} for the most stable conformer (**T1**) are equal to –628.281852 and –628.213369 hartree, respectively.

interconversion between any pair among conformers **T1**, **T2** and **T4** can be achieved through a circular motion around the C–C–C=S axis, while **T3** can be connected to the remaining forms only via **T2** by internal rotation around the C=C–C–C axis. The barriers associated with the **T3** → **T2**, **T2** → **T1**, **T4** → **T2** and **T4** → **T1** were calculated to be 5.8, 8.8, 10.4 and 3.8 kJ mol⁻¹, respectively. As discussed in detail later, the peculiar format of the potential energy profile and the relative values of the energy barriers (and, of course, also the relative energy of the conformers) were found to be the key to the interpretation of the experimental results, in particular to the rationalization for the observation of particular conformers of the thioaldehyde-ketene along the photochemical experiments.

Detailed calculated vibrational data, including potential energy distributions (PED), for the four thioaldehyde-ketene conformers are provided in Tables S1–S5 (Supplementary data). The calculated IR spectra of all four conformers are also shown graphically in Fig. 3. All conformers are predicted to give rise to a band due to the ketene antisymmetric stretching vibration at nearly the same frequency (T1, T2, T4 around 2160 cm⁻¹, T3 at 2135.6 cm⁻¹), so

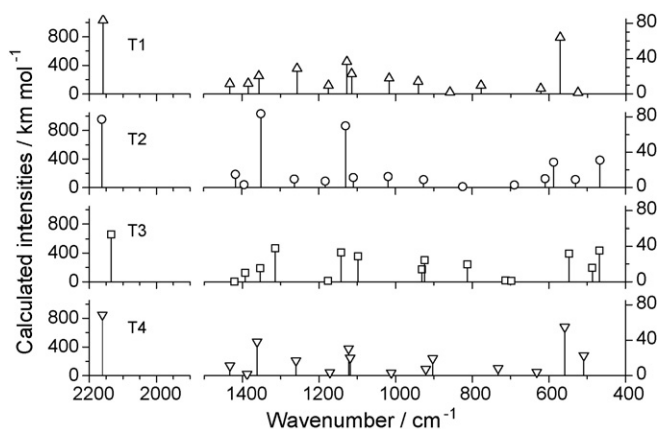


Fig. 3. DFT(B3LYP)/6-311++G(d,p) calculated spectra for the four conformers of the thioaldehyde-ketene isomeric of thiophenone. All calculated wavenumbers were scaled with a factor of 0.978.

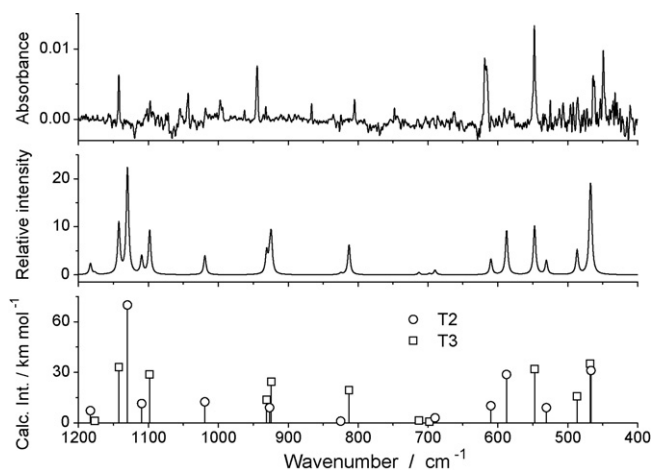


Fig. 4. Upper frame: infrared spectrum of photoproducts generated upon 60 min of UV ($\lambda > 285$ nm) irradiation of matrix-isolated thiophenone monomers. The absorptions of non-reacted thiophenone were nullified as described in the text. Lower frame: DFT(B3LYP)/6-311++G(d,p) calculated infrared spectra for aldehyde-ketene T2 and T3 conformers. The calculated wavenumbers were scaled by 0.978. Middle frame: 1:1 sum spectrum of conformers T2 and T3 simulated using Lorentzian functions with a full width at half maximum (FWHM) of 4 cm⁻¹ and centered on the calculated (scaled) frequencies.

Table 2

Observed experimental infrared absorptions of photoproducts generated after 60 min of UV ($\lambda > 285$ nm) irradiation of thiophenone isolated in an argon matrix at 10 K, and corresponding calculated [DFT(B3LYP)/6-311++G(d,p)] vibrational frequencies (ν , cm^{-1}), infrared intensities (I , km mol^{-1}) and potential energy distributions (PED)

Observed ν	Conf.	Calculated		PED ^b (%)
		ν^a	I	
2136.3	T2	2162.9	954.6	$\nu(\text{C}=\text{O})(68.2) + \nu(\text{C}=\text{C})(31.4)$
2127.9	T3	2135.6	662.4	$\nu(\text{C}=\text{O})(69.3) + \nu(\text{C}=\text{C})(30.1)$
1424.3	T2	1350.6	83.7	$\delta(\text{C}5-\text{H}10)_{\text{as}}(57.6) + \delta(\text{CH}_2)_{\text{wag}}(13.0)$
1380.9	T3	1393.3	10.3	$\delta(\text{CH}_2)_{\text{scis}}(50.3) + \delta(\text{C}3-\text{H}7)_{\text{as}}(13.7) + \nu(\text{C}=\text{C})(13.4) + \nu(\text{C}3-\text{C}4)(12.8)$
1329.3	T3	1314.6	37.8	$\nu(\text{C}4-\text{C}5)(28.4) + \delta(\text{CH}_2)_{\text{wag}}(24.8) + \delta(\text{C}5-\text{H}10)_{\text{as}}(16.0) + \nu(\text{C}3-\text{C}4)(12.1)$
1251.2	T2	1263.5	9.6	$\delta(\text{CH}_2)_{\text{wag}}(58.1) + \nu(\text{C}4-\text{C}5)(14.1) + \delta(\text{C}5-\text{H}10)_{\text{as}}(10.6)$
1141.8	T3	1142.2	33.1	$\delta(\text{C}3-\text{H}7)_{\text{as}}(44.1) + \delta(\text{C}5-\text{H}10)_{\text{as}}(17.4) + \delta(\text{CH}_2)_{\text{wag}}(16.5)$
	T2	1129.9	69.9	$\nu(\text{C}5=\text{S}1)(31.0) + \nu(\text{C}4-\text{C}5)(18.8) + \delta(\text{C}3-\text{H}7)_{\text{as}}(18.2) + \delta(\text{C}5-\text{H}10)_{\text{as}}(13.6)$
1101.8	T3	1098.1	28.8	$\nu(\text{C}5=\text{S}1)(33.9) + \delta(\text{C}3-\text{H}7)_{\text{as}}(22.5) + \delta(\text{C}5-\text{H}10)_{\text{as}}(13.0) + \nu(\text{C}2=\text{C}3)(12.4) + \nu(\text{C}4-\text{C}5)(10.0)$
1018.7	T2	1019.1	12.5	$\nu(\text{C}3-\text{C}4)(37.5)$
944.5	T3	930.9	13.8	$\gamma(\text{C}5-\text{H}10)(54.7) + \delta(\text{CH}_2)_{\text{rock}}(45.7)$
	T2	926.6	9.1	$\gamma(\text{C}5-\text{H}10)(49.1) + \delta(\text{CH}_2)_{\text{rock}}(35.3)$
	T3	924.3	24.5	$\nu(\text{C}3-\text{C}4)(25.3) + \nu(\text{C}5=\text{S}1)(19.9) + \nu(\text{C}2=\text{C}3)(16.8) + \delta(\text{CH}_2)_{\text{wag}}(14.0)$
804.8	T3	813.0	19.5	$\nu(\text{C}4-\text{C}5)(36.7) + \nu(\text{C}3-\text{C}4)(19.9) + \delta(\text{C}2=\text{O})(11.3)$
618.9	T2	587.5	28.7	$\gamma(\text{C}3-\text{H}7)(27.5) + \delta(\text{C}3\text{C}4\text{C}5)_{\text{scis}}(25.9) + \delta(\text{C}5-\text{H}10)_{\text{as}}(21.2)$
547.8	T3	547.5	31.9	$\tau(\text{C}2=\text{C}3)(86.8) + \gamma(\text{C}3-\text{H}7)(16.1)$
524.9	T2	530.7	9.1	$\tau(\text{C}2=\text{C}3)(88.4)$
463.8	T3	486.6	15.9	$\delta(\text{C}2=\text{O})(48.6) + \delta(\text{C}5-\text{H}10)_{\text{as}}(29.6)$
448.8	T3	468.0	35.1	$\gamma(\text{C}3-\text{H}7)(77.9) + \tau(\text{C}2=\text{C}3)(14.4)$
	T2	466.7	31.1	$\gamma(\text{C}3-\text{H}7)(63.4) + \delta(\text{C}5-\text{H}10)_{\text{as}}(16.1)$

^a Theoretical positions of absorption bands were scaled by a factor 0.978.

^b PED's lower than 10% are not included. Definition of symmetry coordinates is given in Table S1 (Supplementary material). See Fig. S1 for atom numbering. s, symmetric; as, antisymmetric; scis, scissoring; wag, wagging; twist, twisting; rock, rocking; ν , stretching; δ , in-plane bending; γ , out-of-plane bending; τ , torsion.

that they can be hardly distinguishable based on the analysis of this spectral region. On the other hand, in the fingerprint region, below 1500 cm^{-1} , the four conformers have quite different spectral signatures, thus opening good perspectives for the characterization of the specific conformer(s) produced upon photolysis of thiophenone.

Fig. 4 shows the spectrum of photoproducts ($1200\text{--}400\text{ cm}^{-1}$ range) generated upon 60 min of UV irradiation with $\lambda > 285$ nm. The absorptions of the non-reacted thiophenone molecules were excluded from the spectra of irradiated samples, by subtracting the spectrum of the non-irradiated matrix from that of the photolysed matrix (with an appropriate scaling factor). Detailed comparison of the fingerprint region of the spectrum of the photolysed matrix with those calculated for the different conformers of the thioaldehyde-ketene allowed us to conclude that conformers **T3** and **T2** are generated in the matrix at the first stage ($\lambda > 285$ nm) of the UV-irradiation process. As it will be shown further in this paper, the ring-opening reaction in 2(5H)-furanone follows the same pattern and the similar photoproducts are formed at this reaction step. This gives us additional confidence in the assignments of the particular conformers in thioaldehyde-ketene photoproducts despite their absorptions in the fingerprint region are intrinsically weak. The proposed assignments of the experimental bands due to the observed photoproducts are given in Table 2.

After 60 min of UV irradiation with $\lambda > 285$ nm, the matrix was subjected to further irradiation with UV light of higher energy ($\lambda > 235$ nm). Already after 30 min of this subsequent irradiation, all remaining thiophenone as well as the initially formed products (**T2** and **T3**) were consumed and new chemical species were formed. Figs. 5 and 6 summarize these results. In the experimental difference spectra shown in these figures, absorptions due to thiophenone were zeroed.

In the $2200\text{--}1700\text{ cm}^{-1}$ spectral range (see Fig. 5), besides changes in the profile of the complex band in the $2140\text{--}2125\text{ cm}^{-1}$ region due to the ketene asymmetric stretching vibration, two new intense bands appear at 2050.3 and 1777.5 cm^{-1} . The first band could be easily assigned to carbonyl sulphide ($\text{O}=\text{C}=\text{S}$) [33,34]. The

second band is ascribed to the carbonyl stretching vibration in the Dewar isomer of thiophenone, 2-thia-bicyclo[2.1.0]pentan-3-one (**TD**). The carbonyl group in **TD** is attached to a four-membered sulphur-containing heterocyclic ring. This four-membered ring is exactly the same in the Dewar isomers originating from both five-membered thiophenone (see Scheme 3) and six-membered thiopyranone (see Scheme 2). Accordingly, the band due to the carbonyl stretching vibration was observed at the same frequency for both species: 1777.5 cm^{-1} (present study), and between 1791 and 1771 cm^{-1} [19]. The theoretical calculations predict that if the carbonyl group is attached to a saturated hydrocarbon ring of varying size, then the carbonyl stretching frequency will increase with the decrease of the ring [35]. Interestingly, this general rule holds also for the conjugated heterocyclic rings, and the $\nu(\text{C}=\text{O})$ vibration for the carbonyl group attached to a 6-membered (thiopyranone), 5-membered (thiophenone) and 4-membered (**TD** analogues) ring is observed at 1672.5 [36], 1713.9 [1] and 1777.5 cm^{-1} (present work), respectively.

The presence of carbonyl sulphide and of the Dewar isomer is confirmed by the observation of other bands fitting well the calculated spectra of **OCS** and **TD** in the fingerprint region (Fig. 6; for the complete set of calculated frequencies and intensities and normal coordinate analysis for **TD** see Tables S6 and S7). The detailed analysis of the fingerprint region of the spectra also allowed us to conclude that conformer **T1** of thioaldehyde-ketene is also generated in matrix by the higher-energy UV irradiation. In the fingerprint region, the strongest band of this form is predicted at around 571 cm^{-1} , between the absorptions of **T2** and **T3** (see Fig. 6). This band does not overlap with absorptions due to other species, and its counterpart is found to appear in the experimental spectrum (at ca. 608 cm^{-1}). Complete assignments of the observed features due to **TD**, **T1** and **OCS** are presented in Table 3.

In summary, irradiation with the $\lambda > 285$ nm light leads to consumption of thiophenone and production of the thioaldehyde-ketene conformers **T2** and **T3**. Subsequent irradiation of the matrix at higher energy ($\lambda > 235$ nm) allows for photoproduction of **TD** and **T1** while thiophenone, **T2** and **T3** are consumed.

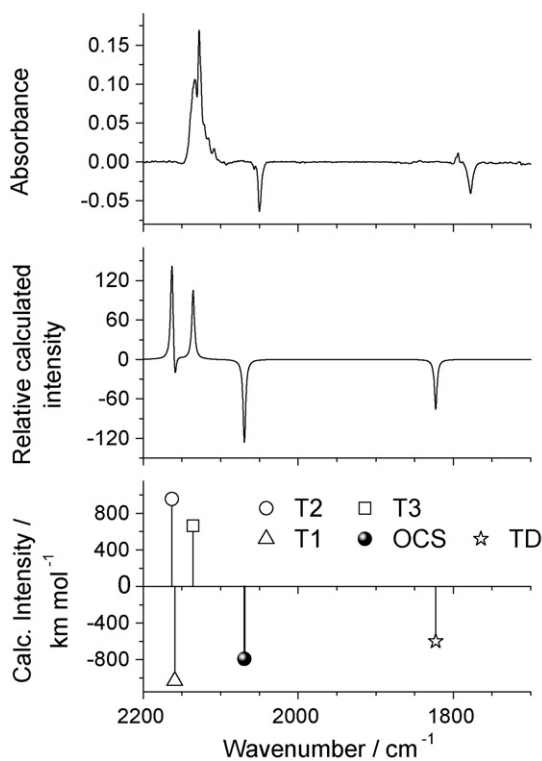


Fig. 5. Upper frame: difference spectrum (2200–1700 cm⁻¹) obtained by subtracting the spectrum of the matrix after photolysis of the matrix at higher energy (30 min, $\lambda > 235$ nm) from that recorded after the first stage of irradiation (60 min, $\lambda > 285$ nm). Bands due to species produced at the first stage have here positive, and those produced at the second stage have negative intensities. Bands due to the reactant (thiophenone) were nullified (see text). Lower frame: B3LYP/6-311+G(d,p) calculated infrared spectra for TD, OCS and the aldehyde-ketene conformers T1, T2 and T3 (wavenumbers scaled by 0.978). The species interpreted as generated at the first stage of photolysis (T2 and T3) have positive intensities (non-scaled), those generated at the second stage of photolysis have negative intensities (scaled by “-1”). Middle frame: simulated spectrum obtained from the calculated spectra shown in the lower frame, using Lorentzian functions with FWHM of 4 cm⁻¹ centered on the calculated (scaled) frequencies and the band intensities scaled for different photoproducts in order to improve the reproduction of the experimental data: “Simulated” = T2+T3–0.3T1–0.8TD–OCS.

The initial generation of **T3** and **T2** is easy to explain. **T3** is the conformer of the thioaldehyde-ketene which requires the minimal spatial rearrangements of the reactant species (thiophenone) upon ring-opening (see the structures of the possible conformers of the

thioaldehyde-ketene shown in Table 1). In addition, among all open-ring conformers, **T3** is the one that requires minimal rearrangements of the matrix cavity which are necessary to accommodate the newly formed species, since, like thiophenone, it has a planar heavy atom skeleton. The presence of **T2** in the irradiated matrix can also be rationalized, considering that **T3** can rearrange thermally to this lower energy conformer, since the barrier for the **T3** → **T2** thermal conversion is low enough (5.8 kJ mol⁻¹). It can be surmounted since the local temperature around the reacting species should be slightly higher than in the remaining matrix bulk due to the energy relaxation, occurring after the photochemical process leading to production of **T3**, which must necessarily involve phonons and participation of the matrix media. It should be noted here, that the barrier for thermal conversion in the reverse direction (**T2** → **T3**) is also relatively low (6.5 kJ mol⁻¹) and the corresponding conversion may also occur in matrices. In view of the fact, that form **T3** has the highest calculated moment among all open-ring conformers, it may undergo additional stabilization in a matrix, so that the difference in energy between **T2** and **T3** is reduced, and accordingly, the barrier heights for the interconversion between these two forms are equilibrated in both directions. Under the condition that one of the two species is generated photochemically, one may expect a thermal relaxation to either **T2** or **T3** with approximately equal probability. Indeed, analysis of the spectral region 650–500 cm⁻¹, where the calculated spectra of **T2** and **T3** differ substantially, suggest that on the first stage of the photoreaction both species are formed (see Fig. 4).

It is also easy to explain why the thermal relaxation of the open-ring compound to its lowest energy conformer **T1** does not take place under these irradiation conditions. Such isomerisation faces much higher barriers comparing to the **T3** → **T2** process. The barrier for the direct **T2** → **T1** transformation is 8.8 kJ mol⁻¹ (see Fig. 2), while isomerisation in the inverse direction, **T2** → **T4** → **T1**, faces even higher barrier (11.2 kJ mol⁻¹) at the first step.

During the second phase of the UV irradiation carried out in this study (higher energy irradiation), **T3** is converted into the Dewar isomer (**Scheme 4**). Indeed, **T3** has the favorable geometrical arrangement for the efficient ring-closure reaction (once the proper energy is available). This process is also expected to be much easier than the putative direct reaction converting thiophenone into **TD**, because this latter, in addition to the reorganization of the ring, would require a simultaneous hydrogen atom migration, contrarily to what happens for the **T3** → **TD** process. Carbonyl sulphide is produced in a subsequent photochemical decomposition of **TD**, in a similar way to what was observed for decomposition of the Dewar isomer of 2*H*-thiopyran-2-one [19] (the six-membered heterocyclic α -carbonyl analogue of thiophenone). Together with OCS, cyclopropene shall be formed, but since its infrared spectrum only contains bands of weak intensity (Table S12), its observation under the present experimental conditions was not possible.

Observation of **T1** can be explained in terms of conversion **T2** → **T1**, when the UV irradiation is performed at higher energy ($\lambda > 235$ nm). Under these conditions, a larger amount of energy must be dissipated, and the local temperature around the reactant species should increase more in relation to the experiment with

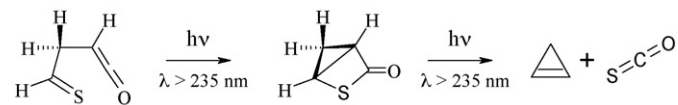


Fig. 6. Changes in the infrared spectra (1200–400 cm⁻¹) of matrix-isolated thiophenone induced by UV irradiation with different cut-off filters. See caption of Fig. 5 for details.

Scheme 4. Observed photochemical reactions leading to conversion of thioaldehyde-ketene **T3** into 2-thia-bicyclo[2.1.0]pentan-3-one (**TD**), cyclopropene and carbonyl sulphide.

Table 3

Observed experimental infrared absorptions of photoproducts generated after 30 min of UV ($\lambda > 235$ nm) irradiation (subsequent to 60 min of irradiation at $\lambda > 285$ nm of thiophenone isolated in an argon matrix at 10 K), and corresponding calculated [DFT(B3LYP)/6-311++G(d,p)] vibrational frequencies (ν , cm^{-1}), infrared intensities (I , km mol^{-1}) and potential energy distributions (PED)

Observed ν	Conf.	Calculated		PED ^b (%)
		ν^a	I	
2130.0	T1	2159.1	1031.7	$\nu(\text{C}2=\text{O}6)(69.7) + \nu(\text{C}2=\text{C}3)(30.0)$
2050.3	OCS	2069.5	793.0	$\nu(\text{O}1=\text{C}2=\text{S}3)_{\text{as}}$
1777.5	TD	1822.6	599.0	$\nu(\text{C}2=\text{O}6)(92.2)$
1455.7	TD	1443.6	6.3	$\delta(\text{CH}_2)_{\text{scis}}(93.7)$
1445.6	T1	1431.6	11.6	$\delta(\text{CH}_2)_{\text{scis}}(97.9)$
1374.5	T1	1383.8	12.0	$\delta(\text{C}3-\text{H}7)_{\text{as}}(24.6) + \nu(\text{C}2=\text{C}3)(22.8) + \delta(\text{CH}_2)_{\text{twist}}(18.9) + \nu(\text{C}5=\text{S}1)(12.2)$
1282.7	T1	1356.2	20.4	$\delta(\text{C}5-\text{H}10)_{\text{as}}(47.9) + \delta(\text{CH}_2)_{\text{wag}}(13.9)$
1257.4	T1	1256.5	28.8	$\delta(\text{CH}_2)_{\text{wag}}(82.2) + \delta(\text{C}5-\text{H}10)_{\text{as}}(13.3)$
1221.2	TD	1210.2	15.2	$\delta(\text{C}5-\text{H}10)(41.0) + \delta(\text{CH}_2)_{\text{twist}}(18.7)$
1119.5	T1	1126.9	36.7	$\delta(\text{C}3-\text{H}7)_{\text{as}}(30.9) + \nu(\text{C}4-\text{C}5)(22.6) + \nu(\text{C}5=\text{S}1)(20.3)$
1104.1	T1	1114.3	22.9	$\delta(\text{C}3-\text{H}7)_{\text{as}}(31.7) + \nu(\text{C}5=\text{S}1)(25.1) + \nu(\text{C}4-\text{C}5)(13.8) + \delta(\text{C}5-\text{H}10)_{\text{as}}(11.5)$
1009.0	TD	1051.6	16.4	$\delta(\text{CH}_2)_{\text{wag}}(30.4) + \gamma(\text{C}3-\text{H}7)(23.4) + \gamma(\text{C}5-\text{H}10)(21.8)$
954.5	T1	941.0	14.1	$\gamma(\text{C}5-\text{H}10)(23.0) + \nu(\text{C}4-\text{C}5)(15.8) + \nu(\text{C}5=\text{S}1)(13.4) + \delta(\text{C}3\text{C}4\text{C}5)_{\text{scis}}(13.1) + \nu(\text{C}3-\text{C}4)(12.3)$
859.0	T1	858.0	2.0	$\nu(\text{C}3-\text{C}4)(28.1) + \delta(\text{CH}_2)_{\text{rock}}(23.2) + \gamma(\text{C}5-\text{H}10)(22.4)$
	OCS	856.5	9.6	$\nu(\text{O}1=\text{C}2=\text{S}3)_{\text{s}}$
839.6	TD	893.3	34.1	$\nu(\text{C}2-\text{C}3)(24.3) + \nu(\text{C}3-\text{C}4)(15.9) + \delta(\text{CH}_2)_{\text{twist}}(12.5) + \delta(\text{CH}_2)_{\text{rock}}(11.0)$
779.9	TD	831.9	47.3	$\nu(\text{C}3-\text{C}4)(32.8) + \gamma(\text{C}5-\text{H}10)(22.4) + \nu(\text{C}4-\text{C}5)(12.0)$
757.0	TD	779.5	30.3	$\nu(\text{C}5-\text{C}3)(34.2) + \delta(\text{C}3-\text{H}7)(21.6) + \nu(\text{C}3-\text{C}4)(11.6)$
753.7				
636.9	TD	598.0	37.2	$\nu(\text{S}1-\text{C}2)(27.0) + \delta(\text{C}2=\text{O}6)(25.3) + \delta_{\text{ring}}(22.1)$
609.0	T1	571.1	64.1	$\gamma(\text{C}3-\text{H}7)(80.9) + \tau(\text{C}2=\text{C}3)(12.6)$
493.9	OCS	500.2	2.7	$\delta(\text{O}1=\text{C}2=\text{S}3)$
		500.2	2.7	$\gamma(\text{O}1=\text{C}2=\text{S}3)$

^a Theoretical positions of absorption bands were scaled by a factor 0.978.

^b PED's lower than 10% are not included. Definition of symmetry coordinates is given in Table S1 for **T1** and in Table S6 for **TD** (Supplementary material). See Fig. S1 for atom numbering. s, symmetric; as, antisymmetric; scis, scissoring; wag, wagging; twist, twisting; rock, rocking; ν , stretching; δ , in-plane bending; γ , out-of-plane bending; τ , torsion.

the lower energy UV irradiation and this appears to be enough to allow for surpassing the ground state barrier between **T2** and **T1**, leading to relaxation of **T2** (which cannot be directly converted to **TD**) to the thioaldehyde-ketene conformational ground state (see Fig. 2).

It is interesting to estimate the relative efficiency of the ring-closure and the open-ring isomerisation processes at the second stage of the UV-irradiation. The relative yield of different photoproducts was adjusted to achieve the best possible fit between the experimentally observed results and the simulated spectra. Such a fit was obtained when both the initial photoproducts (**T2** and **T3**) were consumed in the equal amount, while the secondary photoproducts (**T1**, **TD** and **OCS**) were produced in a proportion 0.3:0.8:1.0, respectively (see Figs. 5 and 6). Since **TD** and **OCS** are formed sequentially in the ring closure reaction channel, it may seem that the ring closure strongly dominates in the unimolecular photochemistry of the open-ring thioaldehyde-ketene species. However, there is a strong misbalance in the amount of the final products (6:1) in favour of **TD** + **OCS**. The expected ratio would be 1:1, assuming that **T1** were formed from **T2** and **TD** from **T3**, with the initial amount of **T2** and **T3** being equal. A plausible explanation to this apparent contradiction is that an efficient conformational isomerisation occurs between the open-ring conformers (in particular, **T2** and **T3**) following the UV excitation. Then the whole population of the reagent should be gradually consumed in the ring-closure photochannel which becomes irreversible upon dissociation of **TD** into **OCS** and cyclopropene.

4.2. Effect of UV irradiation on matrix-isolated 2(5H)-furanone

The infrared spectrum of 2(5H)-furanone (or, for brevity, furanone) monomers isolated in argon matrix was reported in our previous study [1]. The experimental data were compared with

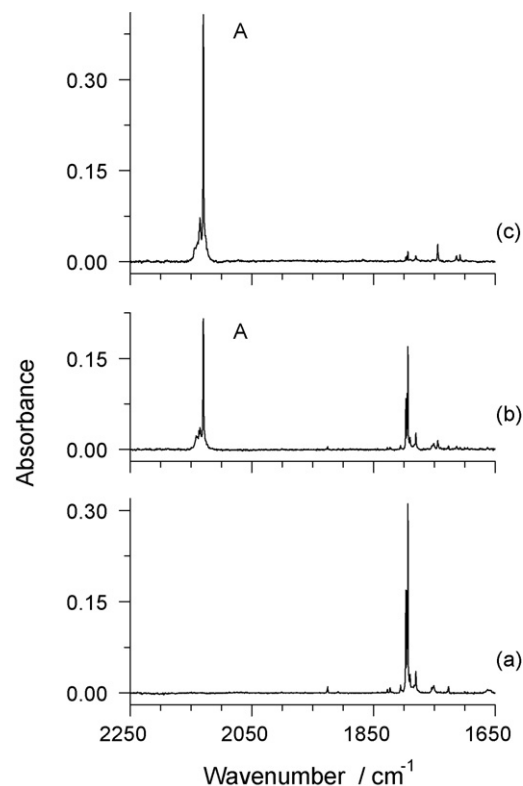
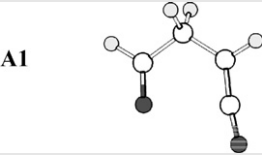
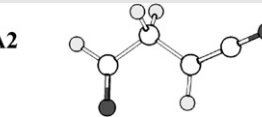
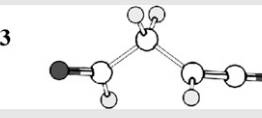
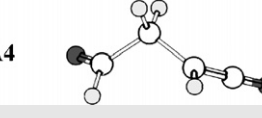


Fig. 7. Region 2200–1650 cm^{-1} of the observed infrared spectrum of 2(5H)-furanone isolated in argon matrix (10 K): (a) as-deposited matrix, (b) after 10 min of UV ($\lambda > 235$ nm) irradiation and, (c) after subsequent 7 min UV ($\lambda > 215$ nm) irradiation. The band due to the reaction product marked with “A” corresponds to open-ring aldehyde-ketene (see text).

Table 4
DFT(B3LYP)/6-311++G(d,p) calculated relative energies (ΔE° , kJ mol⁻¹), zero-point vibrational energy corrected relative energies ($\Delta E^\circ_{\text{ZPVE}}$, kJ mol⁻¹), dipole moments ($|\mu|$, debye), conformer defining dihedral angles (degrees) and symmetry point group of the aldehyde-ketene (A) conformers^a

Conformer	Dihedral angle	Symmetry	ΔE°	$\Delta E^\circ_{\text{ZPVE}}$	$ \mu $
A1 	C=C–C–C: 0.0	C _s	0.0	0.0	4.33
A2 	C–C–C=O: 0.0 C=C–C–C: 180.0	C _s	2.4	1.8	2.54
A3 	C–C–C=O: 0.0 C=C–C–C: 111.1	C ₁	2.7	3.0	1.37
A4 	C–C–C=O: 123.4 C=C–C–C: 103.0	C ₁	5.7	5.5	3.07
	C–C–C=O: –134.6				

^a The calculated values of E° and E°_{ZPVE} for the most stable conformer (**A1**) are equal to –305.325581 and –305.255322 hartree, respectively.

results of theoretical simulations carried out at the DFT(B3LYP) and MP2/6-311++G(d,p) levels of approximation. A very good agreement between the experimental and theoretical spectra allowed for the full assignment of the observed bands.

Similar to thiophenone, furanone monomers isolated in an argon matrix were subjected to a series of UV-irradiations with different longpass filters. Unlike for thiophenone, UV irradiation of furanone at $\lambda > 285$ nm did not induce any changes in the experimental infrared spectra. Only after UV irradiation with an increased energy ($\lambda > 235$ nm and $\lambda > 215$ nm), the changes started to occur. This observation is in agreement with the UV absorption spectra of the two compounds. The lowest energy UV-absorption for thiophenone was experimentally observed at 263 nm (in ethanol) [37,38], while the lowest energy absorption for furanone varies in different solvents [39–41] from 220 nm (in ethanol) [41] to 201 nm (in methanol) [42]. The photoinduced changes in infrared spectrum of matrix-isolated furanone are presented in Fig. 7. UV-irradiation with the $\lambda > 235$ nm light resulted in observation of new bands due to photoproducts, including the characteristic band at ca. 2135 cm⁻¹ due to the antisymmetric stretching vibration of the ketene moiety [19–22,43]. Hence, the ring opening reaction similar to that observed for thiophenone took place under these irradiation conditions. It is worth to mention that irradiation at lower energies was unable to promote any measurable photoreaction, indicating that the ring-opening process in furanone requires considerably more energy than in thiophenone.

For a more precise characterization of the photoproduct ketene, a detailed conformational analysis of the potential energy surface of this species was carried out theoretically. Six minima were located on the PES (Fig. S3), corresponding to four different conformers (two pairs of symmetry-related C₁ conformers and two C_s symmetry unique forms). Like for thiophenone, the furanone conformers were designated by a letter (in this case the letter “A”)

followed by a number increasing in the order of the relative energy of the conformer. The optimized structures for the four different conformers, their symmetry, dipole moment and relative energies are given in Table 4.

The most stable conformer (**A1**; C_s) is identical from two viewpoints to conformer **T3** of thiophenone: it has both conformationally relevant dihedral angles equal to 0 degrees and possesses the highest dipole moment. The second most stable conformer (**A2**) has also its heavy atom backbone planar (C_s) and differs from the most stable conformer by a 180° rotation of the ketene group. Its energy is 2.4 kJ mol⁻¹ higher than that of **A1**. The

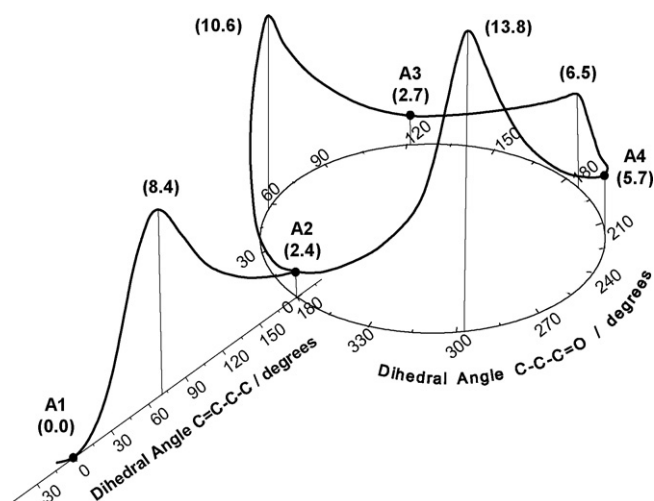


Fig. 8. Calculated potential energy profiles [DFT(B3LYP)/6-311++G(d,p)] for interconversion between the different conformers of aldehyde-ketene open-ring isomer of furanone. Relative energies (kJ mol⁻¹, with respect to form A1) for the stationary points (minima and saddle points on the PES) are given in parentheses.

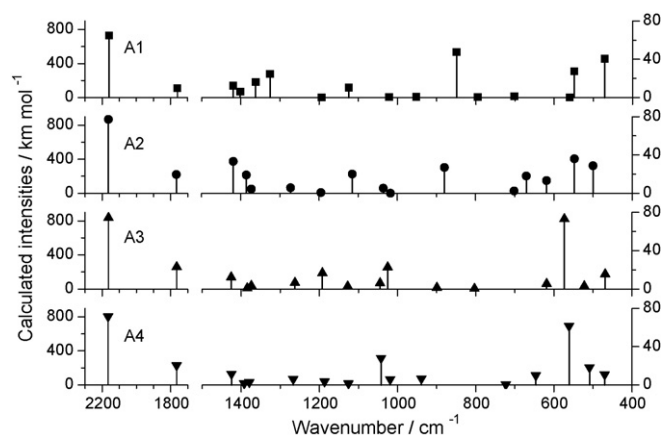


Fig. 9. DFT(B3LYP)/6-311++G(d,p) calculated spectra for the four conformers of the aldehyde-ketene isomer of furanone. All calculated wavenumbers were scaled with a factor of 0.978.

third and fourth conformers (in the energy scale), **A3** and **A4**, are doubly degenerated by symmetry and are analogous to conformers **T1** and **T4** of thiophenone. Their relative energies are respectively 2.7 and 5.7 kJ mol⁻¹ above that of **A1**.

The potential energy profiles for interconversion between the various conformers are presented in Fig. 8. **A1** can be converted to **A2** by internal rotation about the C=C–C–C axis. Interconversion between conformers **A2**, **A3** and **A4** can be accomplished by a circular motion around the C–C–C=O dihedral angle, the barriers for the **A3** → **A2**, **A4** → **A2** and **A4** → **A3** isomerizations being 7.9, 8.1 and 0.8 kJ mol⁻¹, respectively. Globally, the topology of the potential energy surface for the aldehyde-ketene isomer of furanone is similar to that of the thioaldehyde-ketene isomer of thiophenone previously discussed (compare Figs. 8 with Figs. 2). However, in connection with the experiments described in this work, there is an extremely relevant difference: the conformer which can be expected to be the initial product resulting from the ring-opening reaction corresponds to the most stable conformer (**A1**) of the open-ring aldehyde-ketene species. Hence, it can be anticipated that no thermal relaxation to other conformers should take place in the low temperature matrix once **A1** is photolytically generated from furanone. As described below, the experimental data fully confirm this theoretical prediction.

Like for thiophenone, a systematic comparison between the calculated spectra of the different conformers of the aldehyde ketene (Fig. 9; see Tables S8–S11 for full calculated spectra and normal coordinate analysis results) reveals that they are significantly different in the fingerprint region, which can then be used to shed light on the species present in the matrix after irradiation.

Fig. 10 shows the spectra resulting from irradiation of matrix-isolated furanone with the $\lambda > 215$ nm UV light (i.e., with the shortest wavelengths accessible in our experimental setup). Irradiation at higher wavelengths ($\lambda > 235$ nm) led to the qualitatively similar results (see Fig. 7). In particular, no evidence of any additional products was found, though an increased yield of photoreaction was observed for $\lambda > 215$ nm. Comparison of the spectrum of photoproduct(s) with the theoretically predicted spectra for different conformers of the open-ring aldehyde ketene (see Fig. 9) shows that, as expected, the spectrum of the observed photoproduct corresponds to a single ketene conformer, the most stable **A1** form. Assignments for the experimentally observed bands are summarized in Table 5.

As already stressed, for the open-ring isomer of furanone, contrarily to the case of thiophenone, the most stable conformer (**A1**) is expected to be generated in first place upon α -cleavage of the heterocyclic ring. The sole observation of this conformer in the spectrum of the irradiated matrix fully confirms the interpretation of the results presented above for thiophenone. In particular, it is in agreement with the fact that photolysis of both compounds leads to the initial production of the C₅ conformer that has a structure resembling more the heterocyclic precursor molecule, (**A1** and **T3**, for furanone and thiophenone, respectively). In the case of thiophenone, the initially formed open-ring isomer (**T3**) can undergo a subsequent thermal relaxation to other lower energy forms (first to **T2** and, subsequently, to **T1**). In the case of furanone, **A1** is the lowest energy conformer. In the matrix it is likely to be even more stabilized with respect to the other open ring conformers, due to its highest dipole moment. Then **A1** is not further converted to any other species at the matrix temperature.

It must be also reinforced here that for furanone the photochemical reaction leading to the Dewar isomer was not observed, even when UV irradiation was carried out at considerably higher energy comparing to that used in the thiophenone experiments. A simple mechanistic model explaining such observation can be provided by the molecular orbital analysis. The nature of molecular orbitals in the studied compounds was

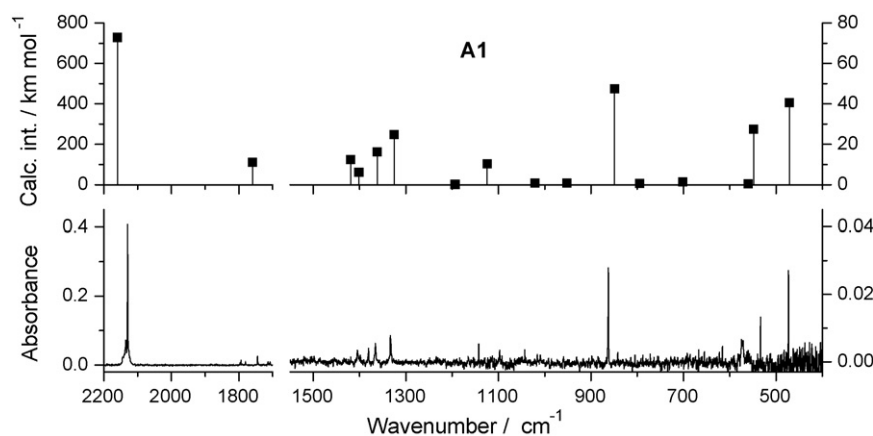


Fig. 10. Lower frame: observed infrared spectrum (2200–400 cm⁻¹ region) of the photoproduct generated upon UV irradiation of matrix-isolated 2(5H)-furanone. Sample was irradiated for 10 min with the $\lambda > 235$ nm light and subsequently for 7 min with the $\lambda > 215$ nm light. The trace bands due to non-reacted furanone (compare with Fig. 7c) were zeroed. Upper frame: DFT(B3LYP)/6-311++G(d,p) calculated infrared spectrum of the open-ring aldehyde-ketene conformer **A1**. The calculated wavenumbers were scaled by 0.978. Note change of the ordinate scale at the abscissa break.

Table 5

Experimentally observed bands of the photoproduct generated after irradiation of furanone isolated in an argon matrix

Observed ν	Conf.	Calculated		PED ^b (%)
		ν^a	I	
2843.7	A1	2848.4	95.0	$\nu(\text{C5-H10})(98.2)$
2135.3	A1	2159.9	728.8	$\nu(\text{C2=O6})(69.8) + \nu(\text{C2=C3})(29.5)$
1744.2	A1	1759.3	110.9	$\nu(\text{C5=O1})(91.3)$
1404.5	A1	1419.2	12.4	$\delta(\text{CH}_2)_{\text{scis}}(79.7)$
1380.7	A1	1401.3	6.1	$\delta(\text{C5-H10})_{\text{as}}(23.8) + \delta(\text{C3-H7})_{\text{as}}(18.7) + \nu(\text{C2=C3})(16.9) + \delta(\text{CH}_2)_{\text{scis}}(14.2) + \nu(\text{C3-C4})(12.8)$
1366.1	A1	1362.0	16.3	$\delta(\text{C5-H10})_{\text{as}}(64.2) + \delta(\text{CH}_2)_{\text{wag}}(11.0)$
1333.2	A1	1325.3	24.8	$\delta(\text{CH}_2)_{\text{wag}}(53.4) + \nu(\text{C4-C5})(16.4) + \nu(\text{C3-C4})(15.8)$
862.3	A1	849.2	47.5	$\nu(\text{C4-C5})(28.7) + \nu(\text{C3-C4})(20.7) + \delta(\text{C5-H10})_{\text{as}}(15.1) + \delta(\text{C2=O6})(12.1)$
572.8	A1	548.5	27.5	$\tau(\text{C2=C3})(91.1)$
472.9	A1	471.0	40.6	$\gamma(\text{C3-H7})(84.2)$

The sample was irradiated for 10 min using UV light with $\lambda > 235$ nm and subsequently for 7 min using UV light with $\lambda > 215$ nm. The corresponding calculated [DFT(B3LYP)/6-311++G(d,p)] vibrational frequencies (ν , cm^{-1}), infrared intensities (I , km mol^{-1}) and potential energy distributions (PED) of the open-ring aldehyde-ketene conformer A1 are shown for comparison.

^a Theoretical positions of absorption bands were scaled by a factor 0.978.

^b PED's lower than 10% are not included. Definition of symmetry coordinates is given in Table S1 (Supplementary material). See Fig. S1 for atom numbering. s, symmetric; as, antisymmetric; scis, scissoring; wag, wagging; twist, twisting; rock, rocking; ν , stretching; δ , in-plane bending; γ , out-of-plane bending; τ , torsion.

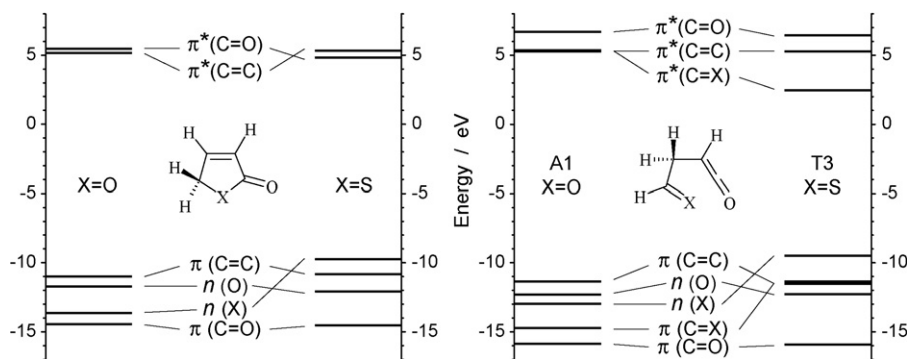


Fig. 11. Energy diagrams of selected Natural Bond Orbitals calculated at the MP2/6-311++G(d,p) level of theory for the two closed-ring compounds (left) and the corresponding open-ring isomeric forms (right). The generalized structures are shown in the centres of diagrams, and the nature of the heteroatom ($\text{X}=\text{O}$, $\text{X}=\text{S}$) is specified aside.

characterized using the natural bond orbital approach [44]. The calculated energies for the frontier molecular orbitals (HOMO and LUMO) as well as for several adjacent orbitals are presented in Fig. 11. The additional orbitals depicted in the figure correspond to all lone electron pairs and to all double-bond π -orbitals.

The left side of Fig. 11 compares orbital energies for the two closed ring species. The relative energies of all orbitals (except one) change only slightly upon $\text{O} \rightarrow \text{S}$ substitution. The exception is the lone electron pair orbital localized on the ring heteroatom (X). The $n(\text{S})$ orbital in thiophenone is strongly destabilized comparing to the $n(\text{O})$ orbital in furanone (see Fig. 11). The substitution of the ring oxygen in furanone by sulphur in thiophenone confers the HOMO character to the $n(\text{S})$ orbital in thiophenone and results in a decrease of the HOMO–LUMO gap. This theoretical finding is in agreement with our experiments showing that UV-induced photochemical transformations in thiophenone start to occur at lower excitation energies comparing to furanone.

The energies of selected molecular orbitals for the two opening isomers are compared in the right side of Fig. 11. The ketene fragment ($\text{C}=\text{C}=\text{O}$) is common for A1 and T3 species, and the orbitals localized at this group have similar relative energies in the two open-ring compounds. On the contrary, the substitution of the $\text{C}=\text{O}$ group by $\text{C}=\text{S}$ group results in a strong destabilization of the $\pi(\text{C}=\text{S})$ and $n(\text{S})$ orbitals, and in the stabilization of the $\pi^*(\text{C}=\text{S})$ orbital, comparing to their oxygen-based analogues. It results in a very pronounced decrease in the HOMO–LUMO gap for the opening thioaldehyde-ketene isomer. This is in agreement with a high photochemical reactivity of thioaldehyde-ketene species observed experimentally.

5. Conclusion

The UV-induced unimolecular photochemistries of 2(5H)-furanone and 2(5H)-thiophenone isolated in low temperature inert argon matrices were studied. FTIR spectroscopy, assisted by quantum chemical theoretical calculations, was used to characterize the photoproducts and shed light on the reaction mechanisms. Both compounds were found to undergo α -cleavage upon UV excitation, though this reaction was found to require considerably more energy in the case of 2(5H)-furanone than for 2(5H)-thiophenone. For the latter molecule, excitation at higher energies leads to conversion of the initially formed thioaldehyde-ketene into the closed-ring Dewar isomer, which subsequently can be decomposed to carbonyl sulphide and cyclopropene. On the other hand, the aldehyde-ketene resulting from the ring-opening reaction of 2(5H)-furanone did not react any further within the whole range of excitation energies used in the present investigation. The different photochemical reactivity experimentally observed for the two families of compounds was explained on the basis of the natural bond orbital analysis carried out at the MP2/6-311++G(d,p) level of theory, which revealed the considerable reduction of the HOMO–LUMO gap in the sulphur containing species.

Acknowledgements

This work was supported by Fundação para a Ciência e a Tecnologia (FCT, Portugal), Grant #SFRH/BD/16119/2004, Projects POCI/QUI/59019/2004 and POCI/QUI/58937/2004, also supported by FEDER.

Appendix A. Supplementary data

Supplementary data associated with this article can be found, in the online version, at [doi:10.1016/j.vibspec.2008.07.015](https://doi.org/10.1016/j.vibspec.2008.07.015).

References

- [1] S. Breda, I. Reva, R. Fausto, *Journal of Molecular Structure* 887 (2008) 75–86.
- [2] A. Yogeve, Y. Mazur, *Journal of the American Chemical Society* 87 (1965) 3520.
- [3] O.L. Chapman, C.L. McIntosh, *Journal of the Chemical Society D: Chemical Communications* (1971) 383.
- [4] A. Padwa, D. Dehm, T. Oine, G.A. Lee, *Journal of the American Chemical Society* 97 (1975) 1837.
- [5] C.D. Gutsche, B.A.M. Oude-Alink, *Journal of the American Chemical Society* 90 (1968) 5855.
- [6] P. Margaretha, P. Schuster, O.E. Polansky, *Tetrahedron* 27 (1971) 71.
- [7] P. Margaretha, *Tetrahedron Letters* (1974) 4205.
- [8] P. Margaretha, *Helvetica Chimica Acta* 57 (1974) 2237.
- [9] P. Margaretha, *Tetrahedron* 29 (1973) 1317.
- [10] P. Margaretha, *Angewandte Chemie-International Edition* 11 (1972) 327.
- [11] R. Kiesewetter, P. Margaretha, *Helvetica Chimica Acta* 72 (1989) 83.
- [12] R. Kiesewetter, P. Margaretha, *Helvetica Chimica Acta* 68 (1985) 2350.
- [13] R. Kiesewetter, A. Graff, P. Margaretha, *Helvetica Chimica Acta* 71 (1988) 502.
- [14] E. Anklam, P. Margaretha, *Angewandte Chemie-International Edition in English* 23 (1984) 364.
- [15] E. Anklam, P. Margaretha, *Helvetica Chimica Acta* 67 (1984) 2198.
- [16] E. Anklam, P. Margaretha, *Helvetica Chimica Acta* 66 (1983) 1466.
- [17] E. Anklam, R. Ghaffaribabrizi, H. Hombrecht, S. Lau, P. Margaretha, *Helvetica Chimica Acta* 67 (1984) 1402.
- [18] Y.S. Rao, *Chem. Rev.* 76 (1976) 625.
- [19] S. Breda, I. Reva, L. Lapinski, M.L.S. Cristiano, L. Frija, R. Fausto, *Journal of Physical Chemistry A* 110 (2006) 6415.
- [20] S. Breda, I. Reva, L. Lapinski, R. Fausto, *Physical Chemistry Chemical Physics* 6 (2004) 929.
- [21] S. Breda, L. Lapinski, R. Fausto, M.J. Nowak, *Physical Chemistry Chemical Physics* 5 (2003) 4527.
- [22] S. Breda, L. Lapinski, I. Reva, R. Fausto, *Journal of Photochemistry and Photobiology A—Chemistry* 162 (2004) 139.
- [23] A.D. Becke, *Physical Review A* 38 (1988) 3098.
- [24] C.T. Lee, W.T. Yang, R.G. Parr, *Physical Review B* 37 (1988) 785.
- [25] S.H. Vosko, L. Wilk, M. Nusair, *Canadian Journal of Physics* 58 (1980) 1200.
- [26] J.H. Schahtschneider, F.S. Mortimer, *Vibrational analysis of polyatomic molecules. VI. FORTRAN IV Programs for Solving the Vibrational Secular Equation and for the Least-Squares Refinement of Force Constants*. Project No. 31450. Structural Interpretation of Spectra, Shell Development Co., Emeryville, CA, 1969.
- [27] M.J. Frisch, G.W. Trucks, H.B. Schlegel, G.E. Scuseria, M.A. Robb, J.R. Cheeseman, J.J.A. Montgomery, T. Vreven, K.N. Kudin, J.C. Burant, J.M. Millam, S.S. Iyengar, J. Tomasi, V. Barone, B. Mennucci, M. Cossi, G. Scalmani, N. Rega, G.A. Petersson, H. Nakatsuji, M. Hada, M. Ehara, K. Toyota, R. Fukuda, J. Hasegawa, M. Ishida, T. Nakajima, Y. Honda, O. Kitao, H. Nakai, M. Klene, X. Li, J.E. Knox, H.P. Hratchian, J.B. Cross, V. Bakken, C. Adamo, J. Jaramillo, R. Gomperts, R.E. Stratmann, O. Yazyev, A.J. Austin, R. Cammi, C. Pomelli, J.W. Ochterski, P.Y. Ayala, K. Morokuma, G.A. Voth, P. Salvador, J.J. Dannenberg, V.G. Zakrzewski, S. Dapprich, A.D. Daniels, M.C. Strain, O. Farkas, D.K. Malick, A.D. Rabuck, K. Raghavachari, J.B. Foresman, J.V. Ortiz, Q. Cui, A.G. Baboul, S. Clifford, J. Cioslowski, B.B. Stefanov, G. Liu, A. Liashenko, P. Piskorz, I. Komaromi, R.L. Martin, D.J. Fox, T. Keith, M.A. Al-Laham, C.Y. Peng, A. Nanayakkara, M. Challacombe, P.M.W. Gill, B. Johnson, W. Chen, M.W. Wong, C. Gonzalez, J.A. Pople, *Gaussian 03, Revision C. 02*, Gaussian, Inc., Wallingford, CT, 2004.
- [28] A.E. Reed, L.A. Curtiss, F. Weinhold, *Chemical Reviews* 88 (1988) 899.
- [29] J.P. Foster, F. Weinhold, *Journal of the American Chemical Society* 102 (1980) 7211.
- [30] S. Breda, I.D. Reva, L. Lapinski, R. Fausto, *ChemPhysChem* 6 (2005) 602.
- [31] L. Lapinski, H. Rostkowska, A. Khvorostov, R. Fausto, M.J. Nowak, *Journal of Physical Chemistry A* 107 (2003) 5913.
- [32] L. Lapinski, M.J. Nowak, A. Les, L. Adamowicz, *Journal of the American Chemical Society* 116 (1994) 1461.
- [33] V.I. Lang, J.S. Winn, *Journal of Chemical Physics* 94 (1991) 5270.
- [34] J.S. Winn, *Journal of Chemical Physics* 94 (1991) 5275.
- [35] H. Hooshyar, H. Rahemi, K.A. Dilmagani, S.F. Tayyari, *Journal of Theoretical & Computational Chemistry* 6 (2007) 459.
- [36] I. Reva, S. Breda, T. Roseiro, E. Eusébio, R. Fausto, *Journal of Organic Chemistry* 70 (2005) 7701.
- [37] A.-B. Hörnfeldt, S. Gronowitz, *Arkiv for Kemi* 21 (1963) 239.
- [38] H.J. Jakobsen, E.H. Larsen, S.-O. Lawesson, *Tetrahedron* 19 (1963) 1867.
- [39] M. Franck-Neumann, C. Berger, *Bulletin De La Societe Chimique De France* (1968) 4067.
- [40] K. Ohga, T. Matsuo, *Bulletin of the Chemical Society of Japan* 43 (1970) 3505.
- [41] J. Brun, M. Dethloff, H. Riebenstahl, *Zeitschrift Fur Physikalische Chemie-Leipzig* 258 (1977) 209.
- [42] J. Gawronski, Q.H. Chen, Z. Geng, B. Huang, M.R. Martin, A.I. Mateo, M. Brzostowska, U. Rychlewska, B.L. Feringa, *Chirality* 9 (1997) 537.
- [43] N. Kus, S. Breda, I. Reva, E. Tasal, C. Ogretir, R. Fausto, *Photochemistry and Photobiology* 83 (2007) 1237.
- [44] F. Weinhold, C.R. Landis, *Valency and Bonding: A Natural Bond Orbital Donor–Acceptor Perspective*, Cambridge University Press, New York, 2005.